Transactions of the KSNVE, 24(3) : 189~197, 2014
http://dx.doi.org/10.5050/KSNVE.2014.24.3.189

한국소음진동공학회논문집 제 24 권 제 3 호, pp. 189~197, 2014
ISSN 1598-2785(Print), ISSN 2287-5476(Online)

[Special Paper]

PowerFLOW Simulation of the Hyundai Simple Model for Sunroof Buffeting

HSM의 썬루프 버페팅을 위한 PowerFLOW 해석

Eui-Sung Choi† and Stephane Cyr*
최 의 성·씨어 스테판

(Received November 19, 2013 ; Revised January 16, 2014 ; Accepted January 16, 2014)

Key Words : PowerFLOW(파워플로), Buffeting(버페팅), Helmholtz Resonator(헬름홀츠 공명기), Vortex Shedding Frequency(와류 발산 주파수)

ABSTRACT

A simplified model in the shape of a wedge box with an opening on the roof was used to generate buffeting conditions at HMC. These measurements performed in controlled conditions are intended to validate the ability of CFD tools to predict buffeting. The results obtained by PowerFLOW are presented in this paper for buffeting and for the boundary layer development on the roof of the model when the roof opening is closed. The flow mechanisms that explain the behavior of the experimental sound pressure level(SPL) curve are described, and an improved setup is used to reproduce the flow structures that lead to the measured SPL.

요 약

윗면에 개구부가 있는 쐐기 상자 모양으로 단순화 된 모델은 현대자동차에서 버페팅 현상을 구현하기 위해 사용되었다. 제안된 조건에서 수행한 측정값들은 버페팅 예측을 통해 CFD의 성능을 검증하기 위함이었다. PowerFLOW를 이용하여 얻어진 버페팅 해석 결과와 개구부가 없는 상태에서의 윗면의 경계층 발달을 이 논문에 기술하였다. 실험에서 측정된 음압은 유동 메커니즘을 통해 기술 하였고, 유동구조를 잘 묘사할 수 있도록 개선된 셋업을 통해 측정된 음압에 근사한 결과를 얻을 수 있었다.

1. Introduction

When buffeting occurs in a passenger vehicle, strong pressure fluctuations inside the cabin are induced by the external flow over an opening of the cabin(sunroof or side-window) creating an unpleasant discomfort to the passengers. The coupling happening between the external flow over the opening and the acoustic behavior of the cabin is well understood and can be measured in a wind-tunnel. But car makers need accurate means

† Corresponding Author ; Member, EXA Korea Ins.
E-mail : eschoi@exa.com
Tel : +82-32-781-3080, Fax : +82-32-781-9080
* EXA Corp.

A part of this paper was presented at the KSNVE 2012 Annual Autumn Conference
‡ Recommended by Editor-in-Chief Weuibong Jung

of simulating buffeting to predict its occurrence and prevent it during the development of vehicles.

During buffeting, the strength of the sound-pressure level(SPL) inside the cabin will depend on several factors such as the size of the opening, its location, the external flow speed and the characteristics of the cabin(leakage, wall stiffness, impedance, etc.). Buffeting has been studied and simulated for some years now and methodologies have been developed to include some of the real world effects(RWE) that influence the SPL during buffeting[1,2].

So on a real car, many factors will influence the results. To stress out the ability of a numerical method to reproduce buffeting, an experiment can be done where many parameters are controlled to minimize their impact. This was done in the past by a group of German car makers[3,4] and this is the approach that was adopted by HMC for this work.

2. Experiment and Simulation

2.1 Experimental Stup

The physical model used for testing was a simple wedge shaped box with and opening on the roof referred to as the Hyundai simple model (HSM). The HSM was made of thick aluminum walls mounted on a metal frame. The inside of the model was padded with absorbing material to change the acoustic response of the cavity. The model was sealed to avoid any leakage flow. The HSM is shown in Fig. 1. The Q-factor of the cavity was evaluated at 10.3 using an acoustic response test(ART).

The model was made to sit on the floor of the wind tunnel. The time history of the pressure inside the model was recorded by a microphone and each pressure time signal was post-treated to get the spectrum. The maximum point of the spectrum and its frequency were extracted for flow velocities ranging between 20 km/h and 100 km/h. Experimental results are presented on Fig. 3 and 4 below.

A second measurement was done at 60 km/h on the roof of the same model with the roof opening closed. The velocity profile was measured at 3 different locations as shown on Fig. 2.

2.2 Buffeting

When an external air stream flows over the opening of a cavity a shear layer is formed. A shear layer is an unstable flow structure that has the tendency to roll up into vortices. These vortices are convected downstream over the opening at a speed slightly below free stream velocity and interact with the trailing edge of the opening. This fluid-structure interaction generates a pressure wave that propagates inside the cavity where it is reflected by the walls. This acoustic wave then

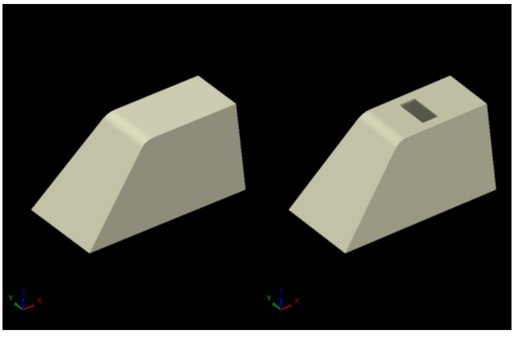

Fig. 1 Configurations of the HSM test in the Hyundai wind-tunnel

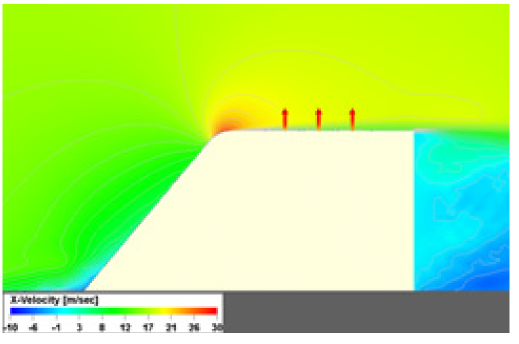

Fig. 2 Positions on the roof where the boundary layer profiles were measured

comes back to the opening to interact with the shear layer[5].

Any cavity with a given opening behaves like a Helmoltz resonator with a given natural frequency. The inside volume of the cavity acts as a spring attached to an equivalent air mass associated with the cavity's opening. The vortex shedding frequency in the shear layer increases linearly with free stream velocity. When the shedding frequency gets closer to the natural frequency of the cavity, a lock-on phenomenon occurs where the acoustic feedback from the cavity initiates the formation of the next vortex in the shear layer. This fluid-acoustic coupling is characterized by an increase of the pressure amplitude in the cavity that is called "buffeting".

As the external velocity is further increased, the shedding frequency becomes larger than the natural frequency of the cavity and the coupling becomes weaker, leading to a decrease of the pressure amplitude inside the cavity. This is the offset phase.

At higher velocities, the shear layer brakes down in smaller vortices that are still interacting with the trailing edge of the opening but over a broader range of frequencies. The cavity is then acoustically excited over a wider range of frequencies but with smaller amplitudes. The sound pressure level is then lower than when buffeting occurs, but it increases with external velocity since the mean momentum of the vortices in the shear layer is proportional to the external velocity.

2.3 Setup and Simulation Procedure

The simulations were performed using PowerFLOW version 4.3b. PowerFLOW is a Lattice Boltzmann method(LBM) based CFD software using a VLES turbulence model. It is a very efficient transient flow solver used by many OEMs(original equipment manufacturer) in the development of car worldwide. The background of the method and the details of its implementation can be found in the references[6~16].

The basic setup was based on the sunroof buffeting best practices recommended by Exa, which was developed and validated with different cars against wind-tunnel measurement. A variable resolution scheme with a minimum cell size of 1.5 mm was used in these simulations. Simulations were done with a symmetry plane and pressure was recorded in the middle of the cavity. Real world effects obtained from the acoustic response test(ART) were implemented in the simulation model to match the acoustic response characteristics of the cabin between test and simulation.

2.4 Simulation Results

Simulations were done for velocities ranging from 20 km/h to 90 km/h.

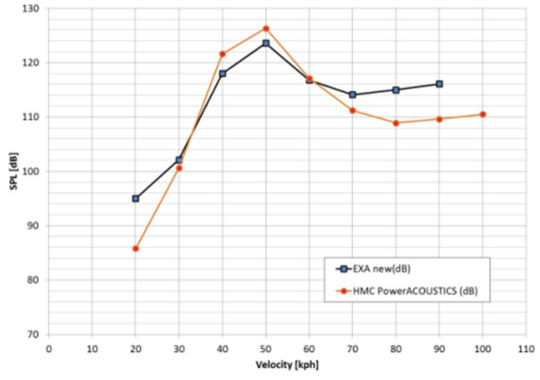

Fig. 3 SPL results with the full Q-factor

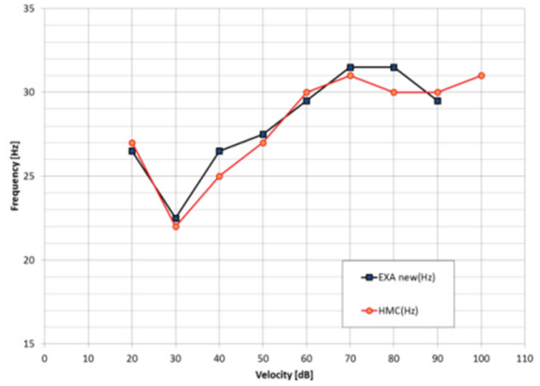

Fig. 4 Frequency results with the full Q-factor

Simulation results are shown in Fig. 3 and 4 for SPL and frequency respectively. The SPL curves show good correlation between test and simulation for the critical velocity range where buffeting occurs. The maximum buffeting occurs at 50 km/h, as in the experiment. SPL for 30 km/h and 60 km/h are at the same level as the experiment. The 40 km/h and 50 km/h SPL are only 4 dB and 2.5 dB lower than experimental values respectively. SPL for velocities above 60 km/h are over predicted by about 6 dB.

The frequency curves show good correlation between test and simulation results. As can be seen on Fig. 4, the buffeting frequency at 60 km/h is nearly on the experimental value. The worst deviation is by 1.5 Hz at 40 km/h and 80 km/h.

Figure 5 shows the pressure signals inside the cavity obtained for different free stream velocities. At the onset of buffeting(30 km/h), the amplitude is low with signs of intermittency. At 50 km/h a strong buffeting is present with a very regular frequency and little modulation of the pressure amplitude. Increasing the free stream velocity to 60 km/h brings the system into the offset mode where strong intermittency shows up again. At 90 km/h the pressure signal becomes more chaotic with small fluctuations immediately followed by strong ones.

So the largest discrepancy exists at higher velocities(70 km/h and above). In this velocity range, the feedback mechanism is not the same as in the buffeting range(40 km/h to 60 km/h). At higher velocities, the acoustic feedback is much less important. The cavity is purely excited by the shear flow interacting with trailing edge of the sunroof opening, and this excitation depends on the structure of the shear flow. Obviously the shear flow obtained in the simulation so far is exciting the trailing edge too much and the maximum SPL in the cavity is too high. Important aspects of shear flow simulation are the boundary layer development of the flow that leads to the shear layer and the possibility of the shear layer to breakdown into smaller vortices.

When analyzed more in depth, the flow around the HSM for this study is trickier than what it can seem at first glance. One peculiar flow structure requires more attention and can turn out to

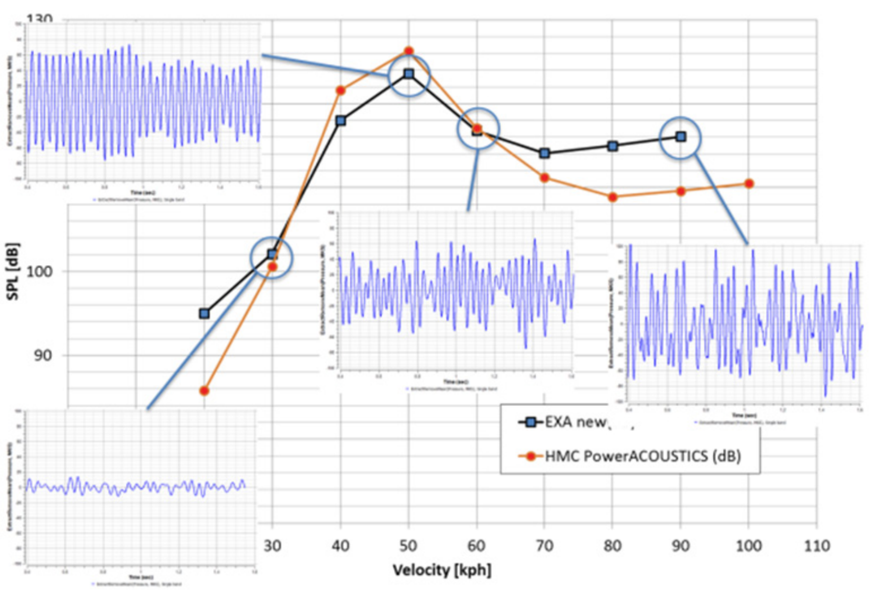

Fig. 5 Simulated pressure time signals at different velocities shown against the SPL curves

improve both the missing SPL at 40 km/h and 50 km/h, and improve the over prediction at higher velocities. This structure is a small flow separation found on the roof right after the slanted front-roof corner. This small flow separation changes the shape of the velocity profile that arrives at the sunroof and influences how the shear layer will develop over the sunroof opening. It was reported by HMC engineers that a flow separation was observed using smoke injection at the roof front corner during the tests in the wind-tunnel.

2.5 Simulation Results - Higher resolution

To better understand the impact of the separation on the shear layer and on the excitation of the cavity, some simulations were done with a higher resolution on the roof and in the shear layer since the size of the flow structures generated in the separation region in front of the sunroof opening are very small. One velocity from the buffeting range(50 km/h) and the offset range(80 km/h) was selected for these higher resolution runs.

At 50 km/h, from the y-plane pictures of vorticity at four different times on Fig. 6, it can be seen that the separation ahead of the opening is intermittent. It shows only on the two last pictures. The four pictures cover a typical cycle of buffeting(about 1/30 sec). In buffeting mode, the shear layer rolls up to create large vortices and the small separation ahead of the opening only creates a small loss of momentum so the vortices interact more strongly with the trailing edge of the opening, and the excitation of the cavity is stronger. The SPL predicted is now exceeding the experimental value by less than 1 dB. If the boundary layer ahead of the opening is not enough resolved, the separation will be over predicted and the momentum loss will be larger. This will lead to a lower excitation of the cavity and a lower SPL. This is what was observed with the lower resolution results presented before.

At 80 km/h, the Reynolds number is higher and the separation region more important. Many small vortices are produced ahead of the opening and convected towards the shear layer. At this velocity the feedback mechanism is not as important as before and the shear layer is composed of many vortices of different sizes. A certain periodic clustering of vortices can be observed in the pictures of Fig. 7 also evenly spaced over a period of 1/30 sec. This shows up as a bump in the pressure spectrum inside the cavity. This is due to a weak acoustic feedback that is still present. But the coherence of the shear flow structures is much less important and the global excitation of the cavity is lower. This is reflected in the lower SPL value.

With the higher resolution, PowerFLOW is able to capture this mechanism and the predicted SPL

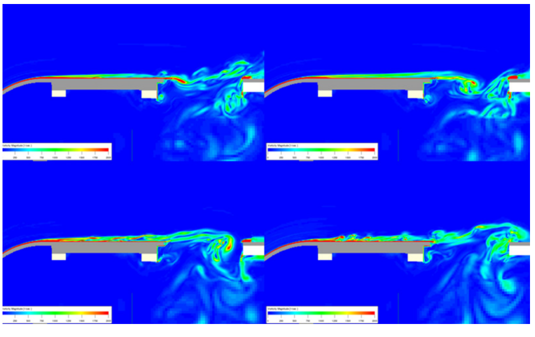

Fig. 6 Y-plane vortices magnitude at 50 km/h with high resolution on front edge

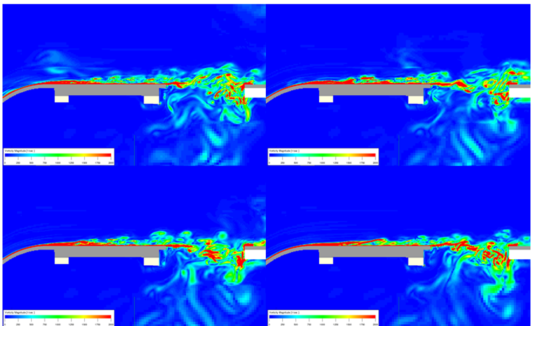

Fig. 7 Y-plane vortices magnitude at 80 km/h with high resolution on front edge

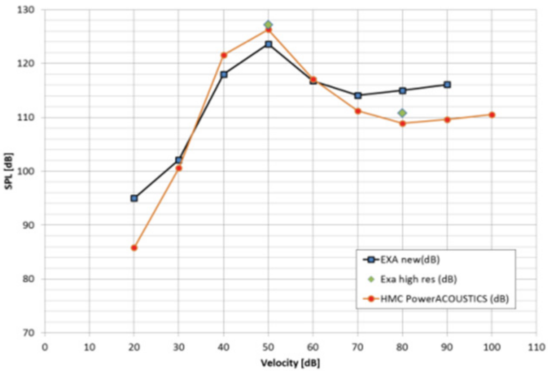

Fig. 8 SPL and frequency for high resolution results for 50 km/h

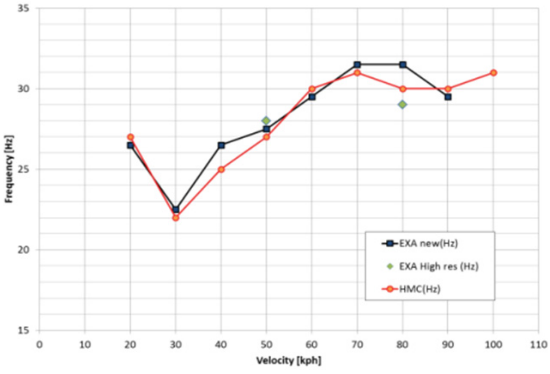

Fig. 9 SPL and frequency for high resolution results for 80 km/h

get very close to the one measured(see Fig. 8 and 9). The 80 km/h SPL value is now only over predicted by less than 2 dB. When the flow is not enough resolved, the vortices coming from the front are larger and the excitation of the cavity also. This is why the SPL was over predicted before.

The frequency at 50 km/h gets slightly higher and at 80 km/h predicted frequency just gets bellow the experimental value. Overall it is an improvement over the previous results.

Because PowerFLOW captured the different mechanisms in buffeting mode and in the offset of buffeting, it is expected that using the higher resolution setup for all velocities would reproduce the experimental values very closely. At 90 km/h

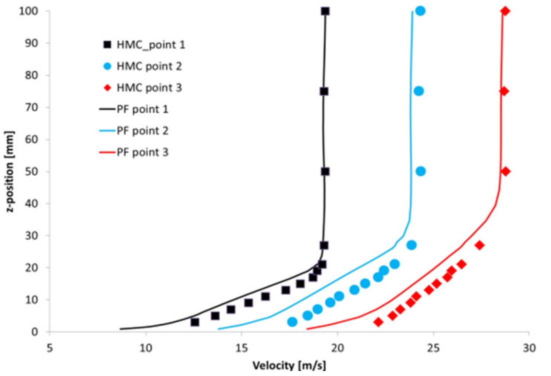

Fig. 10 Comparison of boundary layer profiles(profiles 2 and 3 have been shifted by 5 m/s and 10 m/s for clarity)

and 100 km/h, the vortices in the boundary layer in front of the opening will have the tendency to break down in even smaller structures but their mean convective velocity will be higher and SPL should increase slowly as it is seen with the lower resolution results and as it is seen experimentally.

2.6 Boundary Layer Profiles

The HSM was also simulated with the sunroof opening closed to obtain the boundary layer profile at three locations on the roof with a free stream velocity of 60 km/h(16.67 m/s). The comparison to the experimental velocity profiles is shown in Fig. 10.

The simulated profiles compare well to the experimental measurements at the 3 locations with a slight tendency to underestimate the velocities within the boundary layer. The shapes of the three profiles are identical to the experimental profiles, showing that the flow structures simulated within the boundary layer are reproduced correctly. The underestimation of the velocity within the boundary layer is probably due to a slight over prediction of dissipation in the separation region at the front corner. Ways to improve the results are under investigation. Outside of the boundary layer the comparison to the experimental velocities is very good with errors well within experimental uncertainty.

3. Conclusions

The buffeting behavior of a simple wedge box was tested in the Hyundai wind-tunnel and simulated with PowerFLOW. Peak SPL levels obtained from the simulation correlate well with the test results for the buffeting velocities. Simulation over-predicted the SPL levels for the higher velocities(in the offset region) with the initial setup. By increasing the resolution in the boundary layer in front of the opening, it was demonstrated that results can be improved both in the buffeting range and in the offset of buffeting at higher velocities.

A separation region present just behind the front corner was identified as a key element in determining the SPL over the whole velocity range. At velocities below 60 km/h, the separation is intermittent and does not reduce much momentum close to the surface, leading to high SPL. At velocities above the 60 km/h, the separation is permanent and produces small vortical structures within the boundary layer which results in a much less coherent excitation of the cavity and lower SPL. As observed experimentally.

The velocity profiles of the boundary layer developing over the closed roof configuration compare well to the measurements with a slight tendency to underestimate the velocity within the boundary layer. The velocity prediction outside the boundary layer is very good.

References

(1) Crouse, B., Balasubramanian, G., Senthooran, S., Freed, D., Ih, K. and Shin, S., 2009, Investigation of Gap Deflector Efficiency for Reduction of Sunroof Buffeting, SAE Paper 2009-01-2233.

(2) Crouse, B., Senthooran, S., Balasubramanian, G., Freed, D. and Karbon, K., 2007, Computational Aeroacoustics Investigation of Automobile Sunroof Buffeting", SAE Paper 2007-01-2403.

(3) Islam, M., Decker, F., Hartmann, M., Jäger, A., Lemke, T., Ocker, J., Schwarz, V., Ullrich, F., Schröder, A. and Heider, A., 2008, Investigations of Sunroof Buffeting in an Idealised Generic Vehicle Model – Part 1: Experimental Results, 29th AIAA Aeroacoustics Conference, Paper 2008-2900.

(4) Islam, M., Decker, F., Hartmann, M., Jäger, A., Lemke, T., Ocker, J., Schwarz, V., Ullrich, F., Crouse, B., Balasubramanian, G. and Mendonca, F., 2008, Investigations of Sunroof Buffeting in an Idealised Generic Vehicle Model – Part 2: Numerical Simulations, 29th AIAA Aeroacoustics Conference, Paper 2008-2901.

(5) Kook, H. and Mongeau, L., 2002, Analysis of the Periodic Pressure Fluctuations Induced by Flow Over a Cavity, Journal of Sound and Vibration, Vol. 251, No. 5, pp. 823~846.

(6) Bhatnagar, P., Gross, E. and Krook, M., 1954, A Model for Collision Processes in Gases. I. Small Amplitude Processes in Charged and Neutral One-component System, Physical Review E, Vol. 94, pp. 511~525.

(7) Brès, G., Pérot, F, and Freed, D., 2009, Properties of the Lattice-Boltzmann Method for Acoustics, 30th AIAA Aeroacoustics Conference, Paper 2009-3395.

(8) Chen, H., 1998, Volumetric Formulation of the Lattice Boltzmann Method for Fluid Dynamics: Basic Concept, Physical Review E, Vol. 58, pp. 3955~3963.

(9) Chen, H., Orszag, S., Staroselsky, I. and Succi, S., 2004, Expanded Analogy between Boltzmann Kinetic Theory of Fluid and Turbulence, Journal of Fluid Mechanics, Vol. 519, pp. 307~314.

(10) Chen, H., Teixeira, C. and Molvig, K., 1998, Realization of Fluid Boundary Conditions via Discrete Boltzmann Dynamics, International Journal of Modern Physics C, Vol. 9, No. 8, pp. 1281~1292.

(11) Chen, S. and Doolen, G., 1998, Lattice Boltzmann Method for Fluid Flows, Annual Review of Fluid Mechanics, Vol. 30, pp. 329~364.

(12) Chen, S., Chen, H., Martinez, D. and Matthaeus, W., 1991, Lattice Boltzmann Model for Simulation of Magnetohydrodynamics, Physical Review Letters, Vol. 67, No. 27, pp. 3776~3779.

(13) Li, Y., Shock, R., Zhang, R. and Chen, H.,

2004, Numerical Study of Flow Past an Impulsively Started Cylinder by Lattice Boltzmann Method, Journal of Fluid Mechanics, Vol. 519, pp. 273~300.

(14) Qian, Y., d'Humieres, D. and Lallemand, P., 1992, Lattice BGK Models for Navier-Stokes Equation, Europhysics Letters, Vol. 17, No. 6, pp. 479~484.

(15) Rubinstein, R. and Barton, J. M., 1990, Nonlinear Reynolds Stress Models and the Renormalization Group, Physics of Fluids A, Vol. 2, No. 8, pp. 1472~1476.

(16) Teixeira, C., 1998, Incorporating Turbulence Models into the Lattice-Boltzmann Method, International Journal of Modern Physics C, Vol. 9, No. 8, pp. 1159~1175.

Appendix
(Lattice Boltzmann Method)

The CFD/CAA code PowerFLOW 4.4 is used to compute unsteady flow physics. The code is based on the Lattice Boltzmann method(LBM). Lattice based method were proposed a couple of decades ago as an alternative numerical method to traditional computational fluid dynamics(CFD). Unlike conventional methods based on discretizing the macroscopic continuum equations, LBM starts from "mesoscopic" kinetic equations, i.e. the Boltzmann equation, to predict macroscopic fluid dynamics.

The lattice Boltzmann equation has the following form:

$$f_i(\vec{x}+\vec{ci}\Delta t, t+\Delta t) - f_i(\vec{x},t) = C_i(\vec{x},t) \tag{1}$$

where f_i is the particle distribution function moving in the i^{th} direction, according to a finite set of the discrete velocity vectors $\{c_i,\ i = 0,..b\}$, $c_i \cdot \Delta t$ and Δt are respectively space and time increments. For convenience, we choose the convention $\Delta t = 1$ in the following discussions.

The collision term on the right hand side of Eq. (1) adopts the simplest and most popular form known as the Bhatnagar–Gross–Krook(BGK) :

$$C_i(\vec{x},t) = -\frac{1}{\tau}\left[f_i(\vec{x},t) - f_i^{eq}(\vec{x},t) \right] \tag{2}$$

Here τ is the relaxation time parameter, and f_i^{eq} is the local equilibrium distribution function, which depends on local hydrodynamic properties. The basic hydrodynamic quantities, such as fluid density ρ and velocity u, are obtained through moment summations:

$$\rho(\vec{x},t) = \sum_i f_i(\vec{x},t),\ \rho\vec{u}(\vec{x},t) = \sum_i \vec{c}_i f_i(\vec{x},t) \tag{3}$$

In the low frequency and long-wave-length limit, for a suitable choice of the set of discrete velocity vectors, the transient compressible Navier–Stokes equations are recovered through Chapman–Enskog expansion, in the limit of low Mach numbers (M~0.4). The resulting equation of state obeys the ideal gas law, and the kinematic viscosity of the fluid is related to the relaxation time parameter τ

$$v = \left(\tau - \frac{1}{2}\right)T \tag{4}$$

The combination of Eqs. (1)~(4) forms the usual LBM scheme for fluid dynamics. It is solved on a grid composed of cubic volumetric elements called voxels, and a variable resolution(VR) strategy is allowed, where the grid size changes by a factor of two for adjacent resolution regions.

In order to model the effects of unresolved small scale turbulent fluctuations, the lattice Boltzmann equation is extended by replacing its molecular relaxation time scale with an effective turbulent relaxation time scale, i.e. $\tau \rightarrow \tau_{eff}$, where τ_{eff} is derived from a systematic Renormalization group(RNG) procedure detailed by Chen et al.[(11)]. A turbulent wall-model, including the effect of pressure gradients, is also integrated into the solver. This method is commonly called very large eddy simulation(VLES) and is now validated and productively used for solving a large range of problems such as aerodynamics, thermal, aerospace and aeroacoustics.

Eui-Sung Choi received M.S. in Dept. of mechanical from Hanyang University, Korea in 2003. He is a principal application engineer at Exa Korea working with Automotive OEMs in Korea.

Stephane Cyr received his Ph.D. degree in Mechanical Engineering from McGill University in 1996. He was a professor at the department of Mechanical Engineering at the University of Sherbrooke, Canada for 7 years. In 2003 he joined Exa Corporation working with Automotive OEMs in Europe and Asia in the deployment of numerical solutions in their development process.